DNA-SMART

DNA-SMART: Biopatterned Polymer Film Microchannels for Selective Immobilization of Proteins and Cells

*Ann-Kathrin Schneider, Pavel M. Nikolov, Stefan Giselbrecht, and Christof M. Niemeyer**

***A** novel SMART module, dubbed "DNA-SMART" (DNA substrate modification and replication by thermoforming) is reported, where polymer films are premodified with single-stranded DNA capture strands, microthermoformed into 3D structures, and postmodified with complementary DNA-protein conjugates to realize complex biologically active surfaces within microfluidic devices. As a proof of feasibility, it is demonstrated that microchannels presenting three different proteins on their inner curvilinear surface can be used for selective capture of cells under flow conditions.*

1. Introduction

Miniaturized microfluidic devices play an increasingly important role for culturing, sorting, isolation, and analysis of cells which are considered as critical enabling technologies in molecular and cellular biology, biotechnology, and medicine.[1] Such devices offer many advantages, such as minimal reagent and sample consumption, excellent temperature control, fast processing times, and the option for parallelization thereby enabling the realization of complete lab-on-a-chip systems for isolation, experimental processing, and analysis of living cells.[2–4] For example, microfluidic devices are under development for the capture of circulating tumor cells or other cells of medical interest.[5–10] Furthermore, concave and convex microstructures, such as microfluidic channels are being exploited since many years to mimic vascular structures and to explore how cells respond to geometrical cues.[3,4,11] Such studies have revealed, for instance, that flow conditions, shear stress, and the curvature of fluidic channels significantly affect the growth, morphology, and function of cultured cells in vitro.[12]

Complex microstructures with almost arbitrary 3D shapes are readily available by microthermoforming, which is a microscale polymer molding process wherein clamped thin polymer films are heated above their glass transition temperature into a softened rubber-elastic state and formed to thin-walled microdevices by 3D stretching into an evacuated mold.[13] As a particular advantage, the mild forming conditions of microthermoforming allow one to preserve chemical and structural premodifications of the film material while it is processed by microreplication. This has led to the establishment of SMART (substrate modification and replication by thermoforming) technology, which enables for example the implementation of latent lithographic images into the large-scale production of microdevices bearing complex, bioinspired patterns.[13–15] For instance, in a previously developed SMART module, the site-specific, covalent coupling of a single type of bioactive moieties on defined gray-scale patterns with a lateral resolution of 7.5 µm were produced on the inner curvilinear surfaces of thin film microchannels by a combination of microthermoforming with maskless projection lithography and protein adsorption by photobleaching. These patterns have been validated, amongst other means, by creating 3D cell adhesion patterns of L929 fibroblasts.[16] However, despite the advances in the manufacturing of thin film microdevices, the full exploitation of SMART technology for mimicking vasculatory and other tissue would

A.-K. Schneider, Dr. P. M. Nikolov,
Prof. C. M. Niemeyer
Karlsruhe Institute of Technology (KIT)
Institute for Biological Interfaces (IBG 1)
Hermann-von-Helmholtz-Platz
D-76344 Eggenstein-Leopoldshafen, Germany
E-mail: niemeyer@kit.edu

Dr. S. Giselbrecht
MERLN Institute for Technology-Inspired Regenerative Medicine
Department of Complex Tissue Regeneration
Maastricht University
Universiteitssingel 40 6229
ER Maastricht, PO Box 616, 6200 MD, Maastricht, The Netherlands

DOI: 10.1002/smll.201603923

largely benefit from possibilities to decorate structural premodifications with more than one protein-of-interest in order to resemble and mimic natural systems, such as the extracellular matrix, with a much higher accuracy than conventional techniques.

Biofunctionalization of the surface of microfluidic devices is usually achieved by a homogeneous coating of the device's surface with, for instance, antibodies or other capture reagents to realize specific cell capture.[5–10] To take full advantage of microfluidics in fundamental and applied biomedical cell research, however, the implementation of microarrays of biomolecular capture reagents would be desirable. DNA[17] and protein[18] microarrays on planar surfaces are nowadays established tools in biomedical research for nucleic acid and protein profiling and they have found also their applications in cell biology. For instance, they allow one to screen for binding of cells in a multiplexed fashion,[19,20] to employ different binding interactions mediated by, for example, different antibodies or cell matrix compounds which bind to different targets on a cell surface, as it is necessary to mimic stem cell niches,[21–23] or to present gradients of surface features to cells to enable combinatorial testing of cell-surface interactions.[24,25] While biomolecular microarrays installed on planar surfaces can be integrated into microfluidic systems by hardware solutions, e.g., based on connected reaction chambers, the direct integration of arrays of multiple different protein binders is very difficult to achieve due to their intrinsic instability. This, in turn, calls for mild and regioselective immobilization methods, which are compatible with typical fabrication methods for fluidic microstructures.

To meet these requirements, we here report, for the first time, on the implementation of DNA-surface technology into microthermoforming of polymer films. Our technology, dubbed DNA-SMART, takes advantage of the DNA-directed immobilization (DDI) of proteins and other ligands bearing a single-stranded oligonucleotide tag which can hybridize to complementary surface-bound capture oligonucleotides.[26] Owing to the specificity of Watson–Crick base pairing, many DNA-tagged components can be immobilized simultaneously by self-assembly when sets of orthogonal capture- and tag-oligomer pairs are employed. Importantly, the process of surface microstructuring with stable DNA molecules is therefore separated from surface functionalization with proteins, the latter of which can be conducted under chemically mild, physiological conditions. The DDI method is meanwhile established for fabrication of high-quality protein arrays on flat, 2D substrates which are primarily used for applications in biosensing and cell culture.[27] It is of particular interest that DDI has already been employed by us[28,29] and others[30–33] to decorate planar surfaces with ligand patterns that enable the specific capture, culturing and analysis of living cells. This approach also allows for release of captured cells using a variety of mild cleavage reactions, based on restriction endonucleases,[33] exonuclease digestion, or even strand-exchange reactions. Moreover, DDI enables integration of top-down surface patterning and bottom-up self-assembly of protein-decorated DNA nanostructures, thereby giving access to sophisticated surface architectures wherein the density and nanoscale arrangement of ligands can be tailored to meet specific requirements of adhered cells.[34] We here demonstrate that DDI technology can be implemented into microthermoformed devices by premodification of the polymer films with DNA capture strands in their still planar state and postmodification of the corresponding microthermoformed 3D devices with DNA-protein conjugates. We demonstrate the functionality of the protein-modified 3D microdevices by protein-mediated, selective capture of cells under flow conditions.

2. Results and Discussion

To establish DNA surface functionalization of microthermoformed devices, we initially explored whether protocols for covalent activation of glass surfaces can be adopted to polymer films. Typical procedures for DNA patterning of flat glass surfaces include plasma activation of the solid support, which is then followed by functionalization using organo-trialkoxysilane reagents, such as aminopropyl-triethoxysilane (APTES) and subsequent installment of reactive crosslinkers, bearing for instance *N*-hydroxysuccinimide or epoxy groups.[35] To adopt this chemistry to polymer surfaces, we tested four different commercially available polymer films, polycarbonate (PC), cyclic olefin polymer (COP), polypropylene (PP), and polystyrene (PS), all of which are transparent and have previously been used as materials for microthermoforming and conventional cell culture products.[13,15] Square-cut sheets of these films (about 2×2 cm^2) were subjected to plasma treatment, followed by silanization with APTES and, in case of COP and PC, activation with bis-epoxy-poly(ethyleneglycol) (EPEG) (**Figure 1**A). The substrates were then patterned by ink-jet microdeposition of two different aminoalkyl-derivatized and Cy5-labeled 21-mer oligonucleotides (aF3-Cy5, aF4-Cy5) containing either the coding sequence for immobilization (F3) or a noncoding sequence as negative control (F4). Both oligomers were spotted as adjacently positioned rectangular microarrays, each containing 5×5 spots with an average diameter of ≈200 µm (Figure 1B). Quantification of the Cy5 fluorescence signals (red spots in Figure 1B) indicated that both oligomers were indeed immobilized on the polymer substrates. As judged from the signal intensities (red bars in Figure 1C), oligonucleotide immobilization efficacies were in the same range as those obtained on a glass surface, functionalized under identical conditions. However, efficacies were slightly higher for PC and PP or lower for COP substrates, respectively.

The micropatterned surfaces were then used for immobilization of a Cy3-labeled oligonucleotide (Cy3-cF3) complementary to the immobilized aF3 capture oligomer. Analysis of the Cy3 fluorescence signals (green spots in Figure 1B) revealed that no Cy3 signals were detected on either the noncomplementary capture oligomers aF4 or in the areas surrounding the DNA spots. This observation clearly indicates that probe hybridization exclusively occurred due to specific Watson–Crick base-pairing. A comparative overview of hybridization signals is shown as green bars in Figure 1C. The signals observed for COP were as high as those of glass surfaces while the other materials revealed

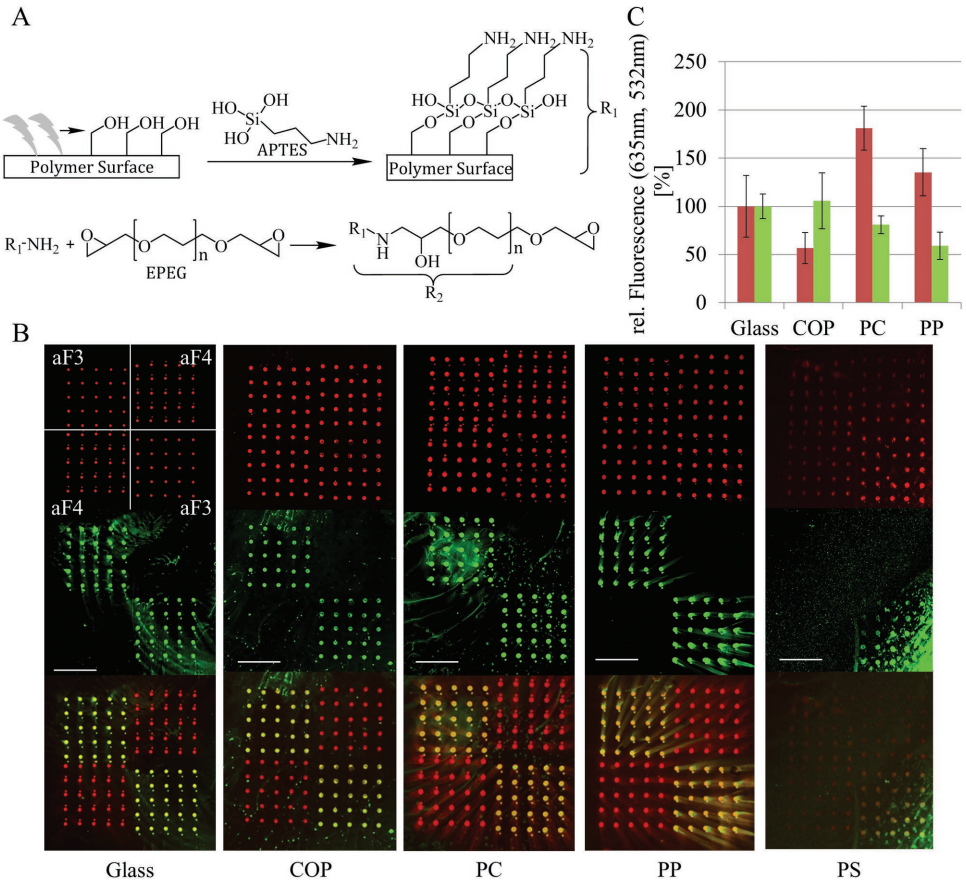

Figure 1. Immobilization and hybridization of oligonucleotides spotted on planar polymer films. A) Polymer surfaces were activated by oxygen plasma treatment and subsequently functionalized using APTES and EPEG to generate reactive groups on the surface for immobilization of amino modified DNA. B) Representative images of Cy5 labeled capture oligomers (aF3, aF4, red dots) spotted as rectangular arrays as indicated in the top left microarray. Hybridization with a Cy3-labeled cF3 oligonuceotide led to formation of green dots. The upper and middle rows show the fluorescence determined at 635 nm (immobilized capture DNA) and 532 nm (hybridized DNA), respectively, the lower row shows the merged images. Scale bars are 2 mm. C) Quantification of fluorescence signal intensities obtained from the images in (B). Signals were normalized to those of the glass surface. The red and green bars represent Cy5- and Cy3-fluorescence signal intensities.

lower fluorescence signals (COP > PC > PP). We observed that PS substrates did not yield reliable hybridization signals (right images, in Figure 1B), presumably due to instable surface attachment of the capture oligomers due to incomplete silanization of the highly hydrophobic PS surface. In contrast, COP revealed highest hybridization efficacies despite the fact that lower amounts of capture probes were present on this material, as compared to PC and PP. Owing to the relatively low hybridization capacity of PP substrates, the further experiments were carried out only with PC or COP substrates.

We then investigated whether DNA-directed immobilization of proteins can be conducted on the DNA-modified polymer films using covalent DNA-streptavidin (DNA-STV) conjugates (**Figure 2**), which were synthesized as previously described.[36] Detailed information on the experimental procedures are provided in the Supporting Information. For an initial test, we coupled DNA-STV conjugate cF9-STV with a biotinylated mouse antibody directed against the cell surface protein VEGFR-2 (vascular endothelial growth factor receptor 2), and the resulting conjugate cF9-STV-αVEGFR2 was allowed to bind to arrays containing the complementary capture oligomer aF9 and the noncomplementary oligomer aF1 (negative control) installed on either COP, PC, or glass substrates. A Cy3-labeled antimouse IgG secondary antibody was used to enable quantification of the fluorescence signals with a microarray scanner. As shown in Figure 2B, bright green spots were observable in regular patterns on the surfaces, indicating both the presence and steric availability of the DNA-IgG conjugates. The absence of fluorescence on the sites containing noncomplementary aF1 oligomers clearly indicated that both the hybridization of cF9-STV-αVEGFR conjugate and the binding of the secondary antibody occurred only due to specific interactions. Quantification of the fluorescence signals (Figure 2C) showed that the binding efficacy of the polymer substrates were comparable with those of the glass substrate. Indeed, COP showed even slightly higher signals than glass and PC and we therefore used exclusively this material for the next steps of our work.

We then tested whether the patterned DNA surface modification can withstand the microthermoforming process. To this end, we designed concave microfluidic channel systems, which can mimic the curvature radii of native vascular structures, such as arterioles and capillaries, and could therefore hold potential for biomedical applications. As illustrated in **Figure 3**, the DNA-modified polymer films were first microthermoformed into half-channel structures. Specifically, the

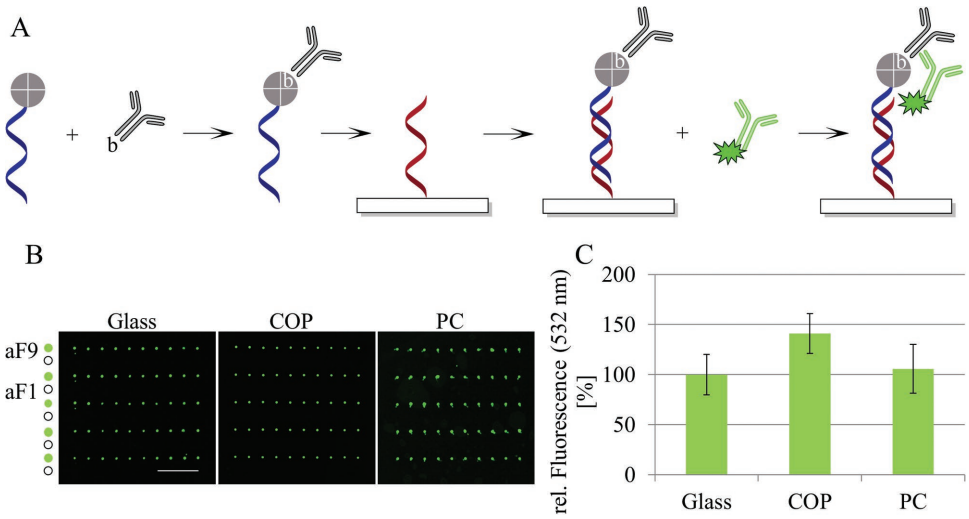

Figure 2. DNA-directed immobilization (DDI) of proteins on the DNA-modified planar polymer films. A) Schematic illustration of the workflow. Binding of a biotinylated VEGFR-2 antibody to the covalent cF9-STV conjugate and subsequent hybridization of the formed conjugate with the immobilized capture oligomer aF1 on the surface. The surface immobilized antibody was visualized with a species-specific Cy3 labeled anti-mouse secondary antibody. B) Capture oligomers aF1 (green spots) and noncomplementary aF9 (indicated by empty circles) were spotted in alternating rows onto functionalized surfaces. Glass served as reference. Binding of the conjugate (cF9-STV-αVEGFR-2) was determined by the Cy3-labeled secondary antibody. Note that no Cy3 signals are visible at the aF1 spots. Scale bars are 2 mm. C) Quantitative fluorescence signal analysis of the microarrays in (B). Signals were normalized to those obtained from the glass surface.

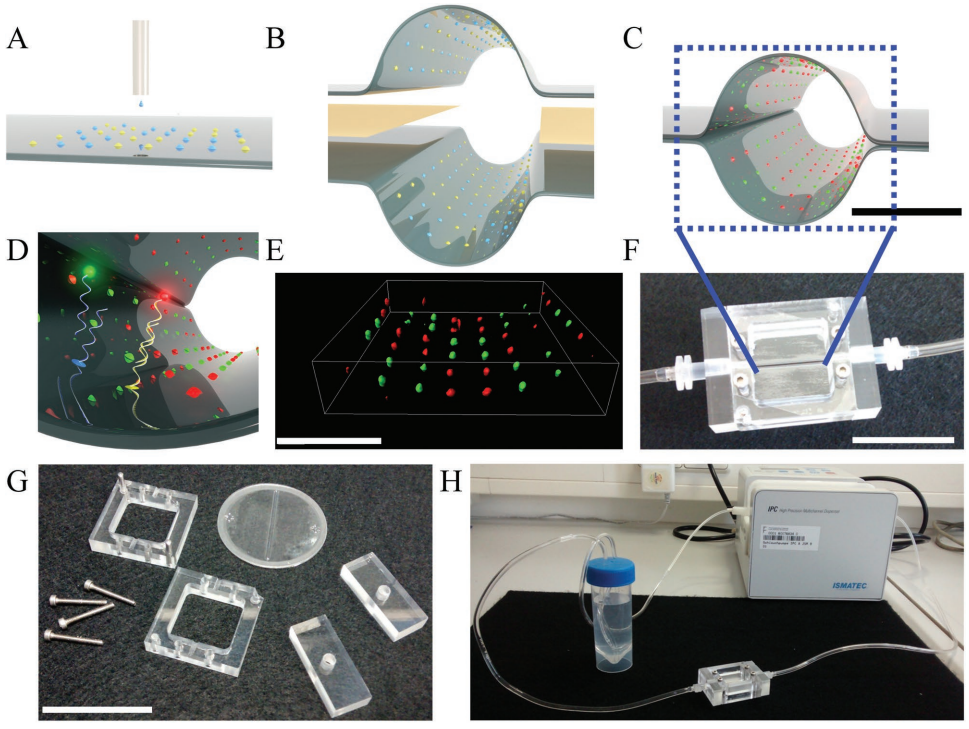

Figure 3. Workflow and technical details of the DNA SMART technology. A) In a preprocess step, the chemically activated thin polymer films bearing epoxy groups were patterned by ink-jet spotting with two different oligonucleotides, indicated by blue and yellow spots. B) The DNA-decorated planar films were then microthermoformed into two half-channels which were then aligned and bonded to create microchannels with a circular cross-section (C, scale bar is 2 mm). The assembled microchannel was then integrated in a microfluidic mount (F, scale bar 250 mm), used to create a standardized chip-to-world interface for connection with a fluidic system where medium is actively pumped from a reservoir through the microchannel by a peristaltic pump in a closed loop circuit (H). G) The image shows the disassembled parts of the mount (scale bar 350 mm). As schematically illustrated in (D), the fluidic system was tested by hybridization of complementary DNA-STV conjugates functionalized with either biotinylated atto550 (green) or biotinylated atto647 (red) under continuous flow conditions. E) 3D image reconstruction of fluorescence images obtained with a confocal laser scanning microscope from a thermoformed microchannel after hybridization with the atto550- (green) and atto647-labeled (red) DNA-STV conjugates (scale bar 500 µm).

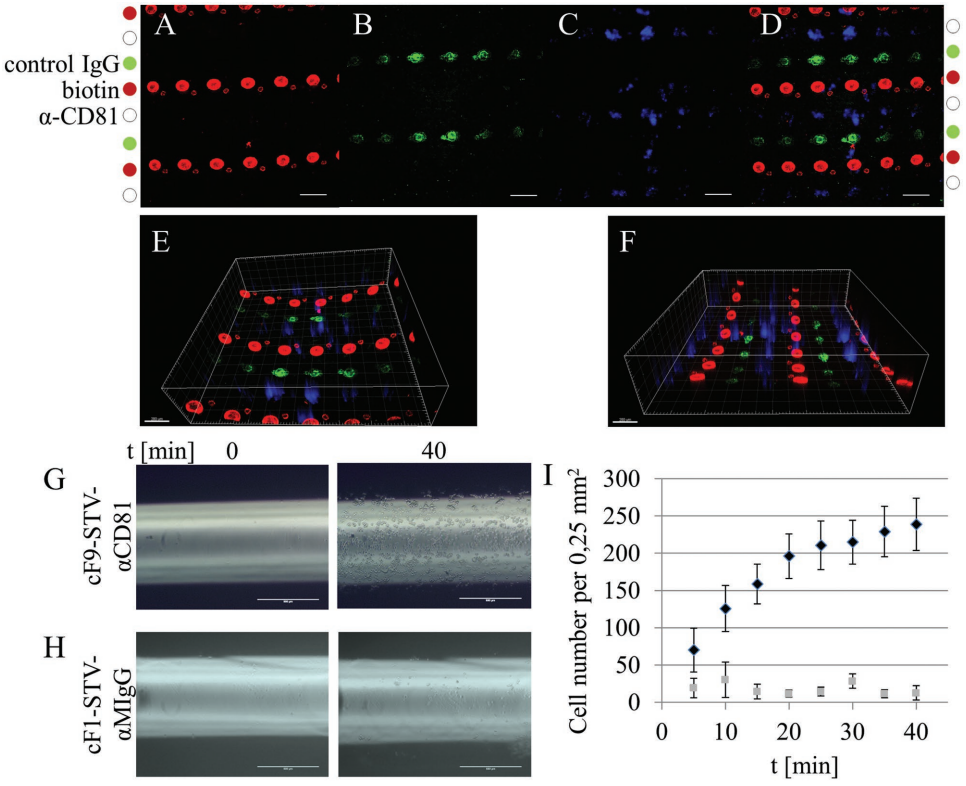

Figure 4. DNA-SMART microchannels with bioactive surface features can be used for specific capture of living cells. An array of oligonucleotides containing Cy3-labeled aF1 (indicated by the green circles), unlabeled aF5 (blank circle) and Cy5-labeled aF9 (red) was spotted onto the epoxy functionalized COP film and thermoformed into a microchannel. The DNA array was then translated into a protein array using the preformed conjugates cF1-STV-αMIgG, cF5-STV-αCD81, and cF9-STV-biotin. Hoechst33342-labeled HEK cells were allowed to adhere to the microchannel's wall under flow conditions for 30 min and fluorescence images were taken. A) Cy5 channel; B) Cy3 channel; C) blue channel to visualize Hoechst staining; D) merged images (all scale bars are 200 µm). Note that cells did only bind to capture spots containing the cF1-STV-αCD81 conjugate (empty circles). The images in (E) and (F) are 3D image reconstructions of the fluorescence images (scale bar: 200 µm). G–I) Time course experiments of selective cell adsorption within the microchannels bearing sections functionalized with conjugates cF9-STV-αCD81 or cF1-STV-αMIgG (scale bar 500 µm).

films were inserted and clamped in a home-built microthermoforming machine.[13] After heating of the COP film to its corresponding forming temperature, which typically is slightly above the glass transition temperature (for details, see the Experimental Section in the Supporting Information), the films were 3D stretched into previously evacuated sheet-like micromolds. The mold was produced by mechanical micromachining and comprised a single central slit-like aperture with a length of 34 mm and a width of 2 mm. The resulting two semicircular microchannels were then aligned and bonded together using a double-sided adhesive tape. By using PDMS (polydimethylsiloxane), the closed microchannel structure was embedded into a microfluidic mount, which served as a standardized chip-to-world interface for connecting the channel with the fluidic peripheral components (Figure 3B,C,F,H). After curing of the PDMS, both ends of the microchannel were cut open to make the channel's lumen accessible. The mount was made from PMMA (polymethylmethacrylate) and consists of a two-part frame to clamp the films and two connector parts containing standard female Luer connectors (Figure 3G).

The fluidic system allows to actively pump buffer or medium from a reservoir through the microchannel by a peristaltic pump in a closed loop circuit. It was used to test the availability of functional DNA capture strands inside the microchannel with a hybridization experiment under continuous flow conditions. To this end, a microchannel patterned with an array of two different oligonucleotides (aF1, aF9) was flushed with a solution containing two complementary DNA-STV conjugates (20×10^{-9} M) labeled with either biotinylated atto550 or biotinylated atto647 dyes (cF9-STV-atto550 and cF1-STV-atto647, respectively). The probes were allowed to bind to the microchannel's wall under a continuous flow rate of 100 µL min^{-1} for 2 h. Subsequently the microchannel was analyzed with a confocal laser scanning microscope. Figure 3E shows a 3D image reconstruction of the fluorescence signals which clearly reveals the micropatterned structure of green and red spots indicating the specific hybridization of the cF9-STV-atto550 and cF1-STV-atto647 probes, respectively, on the inner curvilinear surface of the channel. This result proved that the spotted microarrays of DNA capture strands were preserved upon the thermoforming process and were therefore be usable for immobilization of DNA-protein conjugates.

We then tested whether our DNA-SMART technique allows to prepare microchannels modified with bioactive surface features for specific capture of circulating living cells. For this purpose, a fluidic microchannel containing an array of three different oligonucleotides (Cy3-labeled aF1, unlabeled aF5, and Cy5-labeled aF9) was prepared as described

above and initially functionalized by hybridization of three complementary DNA-STV conjugates (20×10^{-9} M each) for 120 min. Specifically, one conjugate (cF5-STV-αCD81) was prepared from cF5-STV and a biotinylated antibody directed against the cell surface antigen CD81. The second conjugate was prepared from cF1-STV and a biotinylated goat-anti-mouse antibody (cF1-STV-αMIgG) and the third conjugate was cF9-STV, which was saturated with biotin (cF9-STV-biotin, **Figure 4**). The latter two conjugates both served as negative controls for cell capture. Subsequent to DDI of the three STV conjugates, Hoechst 33342-labeled, CD81-positive HEK (Human Embryonal Kidney) cells were allowed to bind to the biopatterned walls of the microchannel under a continuous flow rate of 800 µL min^{-1} for 30 min. Analysis of the channel by fluorescence microscopy (Figure 4A–F) clearly indicated that the specific capture of cells exclusively occurred on spots displaying the αCD81 antibody. In contrast, no cells were observable on the negative control spots or the surrounding area.

The immobilization capacity of the channel is directly proportional to the surface area covered with capture entities. Given the size of spots and array dimensions, about 20% of the surface in the above experiments is indeed presenting the capture reagents (ssDNA and antibodies). Therefore, to increase capture rates in order to evaluate the time dependence of cell capture with our microfluidic device, we used a complete coverage of the channel's inner surface with capture molecules. To this end, a microchannel comprising alternate sections of ≈2 mm length of the two oligonucleotides aF1 and aF9 was prepared as described above and functionalized by hybridization with the conjugates cF9-STV-αCD81 and cF1-STV-αMIgG). HEK cells suspended in PBS (phosphate-buffered saline) were then allowed to bind to the inner channel surface under a constant flow rate of 800 µL min^{-1} for 40 min (Figure 4G,H, see also Figure S1 in the Supporting Information). Microscope images were taken every 5 min and the number of captured cells per 0.25 mm^2 area was counted and plotted against the time (Figure 4I). The results indicated a linear increase of bound cells for ≈20 min which then leveled off and reached a plateau at around 40 min. It is particularly noteworthy that we also confirmed that the immobilized cells are alive and can be further cultured. Subsequent exchange of the buffer with cell culture medium allowed us to culture the adhered cells inside the microchannel for prolonged periods, which led to formation of an almost confluent monolayer of cells (Figure S1C,D, Supporting Information).

3. Conclusion

In summary, we have established the implementation of DNA-surface technology into microthermoforming of polymer films. This DNA-SMART module allows to produce complex patterned 3D thin-walled microdevices, which can be readily functionalized with bioactive proteins by simple flow-through hybridization under mild conditions. We demonstrated that selective immobilization of antibodies gives rise to microchannel structures which can be used for selective binding of living cells. This represents an important advance in the fabrication of fluidic devices for applications in biosensing or in cell culture to mimic vasculature. We would like to emphasize that the employment of DNA surfaces opens up new possibilities for the design of biointerfaces by taking advantage of self-assembled DNA nanostructures.[37] This allows to engineer additional functionality into the bioactive surfaces, such as well-defined nanoscale architectures of ligands to mimic generic properties of the extracellular matrix[34] or switchable units for drug release and adjustment of mechanical properties.

Supporting Information

Supporting Information is available from the Wiley Online Library or from the author.

Acknowledgements

The authors gratefully acknowledge financial support of this work by the Baden-Württemberg Stiftung BioMatS-05 and the Helmholtz programme BioInterfaces in Technology and Medicine. They thank Alex Gerwald for technical support.

[1] C. W. Shields, C. D. Reyes, G. P. Lopez, *Lab Chip* **2015**, *15*, 1230.
[2] F. Lautenschlager, M. Piel, *Curr. Opin. Cell Biol.* **2013**, *25*, 116.
[3] D. Kim, X. Wu, A. T. Young, C. L. Haynes, *Acc. Chem. Res.* **2014**, *47*, 1165.
[4] A. Reece, B. Xia, Z. Jiang, B. Noren, R. McBride, J. Oakey, *Curr. Opin. Biotechnol.* **2016**, *40*, 90.
[5] S. Nagrath, L. V. Sequist, S. Maheswaran, D. W. Bell, D. Irimia, L. Ulkus, M. R. Smith, E. L. Kwak, S. Digumarthy, A. Muzikansky, P. Ryan, U. J. Balis, R. G. Tompkins, D. A. Haber, M. Toner, *Nature* **2007**, *450*, 1235.
[6] S. L. Stott, C. H. Hsu, D. I. Tsukrov, M. Yu, D. T. Miyamoto, B. A. Waltman, S. M. Rothenberg, A. M. Shah, M. E. Smas, G. K. Korir, F. P. Floyd, A. J. Gilman, J. B. Lord, D. Winokur, S. Springer, D. Irimia, S. Nagrath, L. V. Sequist, R. J. Lee, K. J. Isselbacher, S. Maheswaran, D. A. Haber, M. Toner, *Proc. Natl. Acad. Sci. USA* **2010**, *107*, 18392.
[7] X. Zheng, L. Jiang, J. Schroeder, A. Stopeck, Y. Zohar, *Biomicrofluidics* **2014**, *8*, 024119.
[8] J. H. Myung, S. Hong, *Lab Chip* **2015**, *15*, 4500.
[9] T. Yeo, S. J. Tan, C. L. Lim, D. P. Lau, Y. W. Chua, S. S. Krisna, G. Iyer, G. S. Tan, T. K. Lim, D. S. Tan, W. T. Lim, C. T. Lim, *Sci. Rep.* **2016**, *6*, 22076.
[10] D. Yang, S. Leong, A. Lei, L. L. Sohn, *Proc. SPIE Int. Soc. Opt. Eng.* **2015**, 9518.
[11] J. Y. Park, D. H. Lee, E. J. Lee, S. H. Lee, *Lab Chip* **2009**, *9*, 2043.
[12] M. B. Esch, D. J. Post, M. L. Shuler, T. Stokol, *Tissue Eng. Part A* **2011**, *17*, 2965.
[13] R. Truckenmuller, S. Giselbrecht, N. Rivron, E. Gottwald, V. Saile, A. van den Berg, M. Wessling, C. van Blitterswijk, *Adv. Mater.* **2011**, *23*, 1311.
[14] S. Giselbrecht, T. Gietzelt, E. Gottwald, C. Trautmann, R. Truckenmuller, K. F. Weibezahn, A. Welle, *Biomed. Microdevices* **2006**, *8*, 191.
[15] S. Giselbrecht, M. Reinhardt, T. Mappes, M. Borner, E. Gottwald, C. van Blitterswijk, V. Saile, R. Truckenmuller, *Adv. Mater.* **2011**, *23*, 4873.

[16] B. Waterkotte, F. Bally, P. M. Nikolov, A. Waldbaur, B. E. Rapp, R. Truckenmüller, J. Lahann, K. Schmitz, S. Giselbrecht, *Adv. Funct. Mater.* **2014**, *24*, 442.
[17] A. Sassolas, B. D. Leca-Bouvier, L. J. Blum, *Chem. Rev.* **2008**, *108*, 109.
[18] P. Jonkheijm, D. Weinrich, H. Schroeder, C. M. Niemeyer, H. Waldmann, *Angew. Chem., Int. Ed.* **2008**, *47*, 9618.
[19] T. G. Fernandes, M. M. Diogo, D. S. Clark, J. S. Dordick, J. M. Cabral, *Trends Biotechnol.* **2009**, *27*, 342.
[20] F. Brinkmann, M. Hirtz, A. Haller, T. M. Gorges, M. J. Vellekoop, S. Riethdorf, V. Muller, K. Pantel, H. Fuchs, *Sci. Rep.* **2015**, *5*, 15342.
[21] C. J. Flaim, S. Chien, S. N. Bhatia, *Nat. Methods* **2005**, *2*, 119.
[22] Y. Soen, A. Mori, T. D. Palmer, P. O. Brown, *Mol. Syst. Biol.* **2006**, *2*, 37.
[23] M. A. LaBarge, C. M. Nelson, R. Villadsen, A. Fridriksdottir, J. R. Ruth, M. R. Stampfer, O. W. Petersen, M. J. Bissell, *Integr. Biol. (Camb.)* **2009**, *1*, 70.
[24] N. D. Gallant, J. L. Charest, W. P. King, A. J. Garcia, *J Nanosci. Nanotechnol.* **2007**, *7*, 803.
[25] T. Satav, J. Huskens, P. Jonkheijm, *Small* **2015**, *11*, 5184.
[26] C. M. Niemeyer, T. Sano, C. L. Smith, C. R. Cantor, *Nucl. Acids Res.* **1994**, *22*, 5530.
[27] R. Meyer, S. Giselbrecht, B. E. Rapp, M. Hirtz, C. M. Niemeyer, *Curr. Opin. Chem. Biol.* **2014**, *18C*, 8.
[28] H. Schroeder, B. Ellinger, C. F. W. Becker, H. Waldmann, C. M. Niemeyer, *Angew. Chem., Int. Ed.* **2007**, *46*, 4180.
[29] S. Reisewitz, H. Schroeder, N. Tort, K. A. Edwards, A. J. Baeumner, C. M. Niemeyer, *Small* **2010**, *6*, 2162.
[30] R. C. Bailey, G. A. Kwong, C. G. Radu, O. N. Witte, J. R. Heath, *J. Am. Chem. Soc.* **2007**, *129*, 1959.
[31] U. Vermesh, O. Vermesh, J. Wang, G. A. Kwong, C. Ma, K. Hwang, J. R. Heath, *Angew. Chem., Int. Ed. Engl.* **2011**, *50*, 7378.
[32] Q. Shi, L. Qin, W. Wei, F. Geng, R. Fan, Y. Shik Shin, D. Guo, L. Hood, P. S. Mischel, J. R. Heath, *Proc. Natl. Acad. Sci. USA* **2012**, *109*, 419.
[33] R. Bombera, L. Leroy, T. Livache, Y. Roupioz, *Biosens. Bioelectron.* **2012**, *33*, 10.
[34] A. Angelin, S. Weigel, R. Garrecht, R. Meyer, J. Bauer, R. K. Kumar, M. Hirtz, C. M. Niemeyer, *Angew. Chem., Int. Ed. Engl.* **2015**, *54*, 15813.
[35] M. C. Pirrung, *Angew. Chem., Int. Ed.* **2002**, *41*, 1276.
[36] R. Wacker, C. M. Niemeyer, in *Current Protocols in Nucleic Acid Chemistry*, Vol. Suppl. *21* (Ed.: D. E. Bergstrom), John Wiley & Sons, NJ, USA **2005**, p. 12.7.1.
[37] U. Feldkamp, C. M. Niemeyer, *Angew. Chem., Int. Ed.* **2006**, *45*, 1856.

Received: November 23, 2016
Revised: January 18, 2017
Published online: February 22, 2017

